

Calculation of electron states in $\text{Cu}_x\text{Zr}_{1-x}$ glasses by the orthogonalized linear combination of atomic orbitals method

W. Y. Ching and L. W. Song

Department of Physics, University of Missouri—Kansas City, Kansas City, Missouri 64110

S. S. Jaswal

Behlen Laboratory of Physics, University of Nebraska, Lincoln, Nebraska 68588

(Received 12 December 1983; revised manuscript received 26 March 1984)

Based on periodic structural models containing 90 atoms which are computer relaxed, the electronic structures of metallic glasses $\text{Cu}_x\text{Zr}_{1-x}$ are calculated using a first-principles orthogonalized linear combination of atomic orbitals method. The calculated density-of-states curves and their values at the Fermi level are in good agreement with experiments. Each electronic state in $\text{Cu}_x\text{Zr}_{1-x}$ is analyzed in terms of a localization index. It is shown that the Cu states are localized and the Zr states are relatively delocalized. The states at the Fermi level are delocalized but there is a tendency for a slight increase in their localization index when the Cu concentration is increased. The implications of these results for the transport properties of metallic glasses are discussed.

I. INTRODUCTION

Metallic glasses are one of the most important systems in the general area of disordered condensed matter physics. Over the past few years metallic glasses have received a great deal of experimental attention, especially in characterizing their structural, mechanical, electrical, magnetic, and superconducting properties.^{1,2} While enormous amounts of data have been accumulated, their interpretation and explanation in terms of a consistent theory has not been fully realized. Ziman's theory³ and its extensions,^{4,5} which are quite successful in the case of liquid metals, have met with only limited success in metallic glasses¹ and it is still a puzzle why such a theory, which is essentially based on a nearly-free-electron model, should be applicable to strong scattering systems such as those involving transition-metal d electrons. One of the key elements required to formulate a better theory is a fuller understanding of the electronic structures of various metallic glass systems. Although the calculation of band structures of crystalline metals has been advanced to a stage of high sophistication, realistic calculations of electron states in metallic glasses are only beginning. Generally speaking, there are three levels of information about the electronic structures of metallic glasses: (1) the electron density of states (DOS), which is the most fundamental quantity describing the electron states in a disordered solid; (2) the value of the DOS at the Fermi level E_f , which relates to so many important experimentally measurable parameters, such as the superconducting temperature T_c , the temperature coefficient of specific heat and magnetic susceptibility, and which enables an accurate estimation of the effects of spin fluctuations; (3) the nature of electronic states at E_f , particularly the degree of localization, which is related to the electronic mean free path and is critical to the interpretation of many anomalies in the transport properties of metallic glasses.

Current theoretical efforts concentrate on obtaining the DOS curves,⁶⁻¹² which can then be compared with photoemission experiments. In this paper we describe the methods and the results of a calculation on $\text{Cu}_x\text{Zr}_{1-x}$ glasses, which provides the three above-mentioned levels of information. In recent years, the $\text{Cu}_x\text{Zr}_{1-x}$ metallic glass series has been studied in detail experimentally.¹³⁻²⁵ This glass, which consists of an early transition (ET) metal Zr and a late transition (LT) metal Cu, can be formed in a wide range of compositions and exhibits many interesting properties such as superconductivity,^{14,15,17,22} negative temperature and pressure coefficients of electric resistivity,^{16,19,20,25} and crossover behavior of the Hall coefficient.^{13,16} Our approach to the calculation of the electronic structures in $\text{Cu}_x\text{Zr}_{1-x}$ is as follows. First, we construct appropriate structural models consisting of 90 atoms in a cubic cell, which are periodically extended. We then apply a first-principles method, the orthogonalized linear combination of atomic orbitals (OLCAO) method,²⁶ to obtain the electronic structures. Next, we analyze the resulting wave functions of each state in terms of a localization index (LI) to reveal its degree of localization. Our previous work²⁷ on this system involves only 39 atoms in the periodic cell and therefore is too small to analyze the wave functions in terms of its LI. It must be pointed out that the first-principles nature of the calculation and the use of a sufficiently large quasiunit cell are essential in making meaningful localization analyses. In empirical studies the interaction matrix elements are usually parameterized and do not fully reflect the random potential field experienced by an electron in a disordered solid; hence in these studies a similar type of localization analysis will be unreliable, if not impossible. The present paper is organized as follows. In Sec. II the construction of model structures used in the present calculation is described. The essential steps of the theoretical calculation of electron states are outlined in Sec. III. The results

are presented in Sec. IV, where comparisons with relevant experiments and other calculations are made. The last section is devoted to a discussion and some concluding remarks.

II. CONSTRUCTION OF STRUCTURAL MODELS

Before actual construction of the model, we must first decide the total number of atoms N (both Cu and Zr) to be included in the cubic cell. One would like to have N as large as possible, limited only by one's computational resources. Since our aim is to study the electronic structures, N is determined by the feasibility of performing an electronic structure calculation using the method to be described in the next section. We chose N to be 90 for calculation with $\text{Cu}_x\text{Zr}_{1-x}$. The second step is to determine the size of the cubic cell. This is done by requiring the mass density of the model to be the same as the experimentally determined values. In Fig. 1 we plot the measured densities of $\text{Cu}_x\text{Zr}_{1-x}$ which appeared in the literature²⁸⁻³¹ as a function of x , and use this curve to determine the size of the cubic cell at any value of x . For a given value of x , an appropriate number of Cu atoms and Zr atoms are placed at random in the cubic cell. This initial configuration of the model must be relaxed under a suitable potential field. Following several workers in the field,³²⁻³⁴ we use a Lennard-Jones type of potential of the form

$$U_{ij} = \begin{cases} \frac{A}{r_{ij}^{12}} + \frac{B}{r_{ij}^6} + Cr_{ij} + D & \text{for } 0 < r_{ij} \leq r_t, \\ 0 & \text{for } r_t > r_{ij}, \end{cases} \quad (1)$$

where r_{ij} is the distance of separation between the atoms i and j , and r_t is the truncation distance which is set rather arbitrarily. The parameters A and B are generally fixed by the available experimental information such as interatomic separation, cohesive energy, and bulk compressibility of the elemental metal. (The parameters for the Cu-Zr pair are taken as the geometric means of the Cu-Cu and Zr-Zr pairs.) The parameters C and D are fixed by the condition that U_{ij} and its derivative vanish at r_t . These parameters are listed in Table I and the three types of the pair-wise potentials are plotted in Fig. 2. Two types of relaxation processes are used: (1) the conjugate gradient method,³⁵ in which each atom moves in turn to the position of zero force field under the potential given by Eq. (1) until the total elastic energy can no longer be reduced; this corresponds to the case of zero-temperature quenching; and (2) the Monte Carlo method, in which a fictitious temperature parameter T is introduced; the sys-

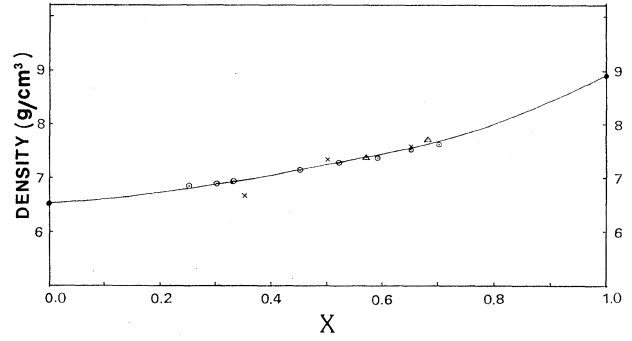


FIG. 1. Density of $\text{Cu}_x\text{Zr}_{1-x}$ as a function of x . \odot denotes Ref. 29; \triangle denotes Ref. 28; \times denotes Ref. 27.

tem is then relaxed using the conventional Monte Carlo algorithm³⁶ by successively reducing the "temperature" T from an initial high value down to zero. There appears to be no significant difference in the radial distribution function of the same model relaxed by the above two different methods, but the Monte Carlo method gives a faster rate of convergence towards the final equilibrium configuration. Furthermore, the Monte Carlo method of statistical mechanics bears a close resemblance to the actual rapid-quenching process in the preparation of metallic glasses.

Throughout the relaxation process, periodic nearest-neighbor boundary conditions were imposed and all the pair-wise interactions for pairs of atoms within a distance r_t are included. The pair correlation function (PCF)

$$W(r) = 4\pi[\rho(r) - \rho_0]/\rho_0, \quad (2)$$

is then calculated from the resulting equilibrium positions of the atoms where ρ_0 is the average atomic density. These are shown in Figs. 2-5 for the three values of x considered: $x = 0.33$, $x = 0.50$, and $x = 0.67$. Also shown are the experimentally determined PCF for comparison.^{28,29} The two methods of relaxation gave similar results and the agreement with the experimental curves^{28,29} is quite reasonable. The slight differences in the small substructures of PCF can be attributed to the simplified potential functions used in the relaxation and the limited number of atoms per cubic cell considered. A more realistic interatomic potential in metallic systems should include Friedel oscillations in the tail part of the potential.³⁷ However, other than the case of simple metals,³⁸ it is quite difficult to derive more general and accurate potential functions either from first principles or from experimental data. We have also calculated the average nearest-neighbor coordination numbers Z_{Cu} and

TABLE I. Parameters of modified Lennard-Jones potential interatomic distances and truncation distances used in the relaxation of structure models for $\text{Cu}_x\text{Zr}_{1-x}$.

Pair	A ($\text{eV} \text{ \AA}^{12}$)	B ($\text{eV} \text{ \AA}^6$)	C ($\text{eV} \text{ \AA}^{-1}$)	D (eV)	R_0 (\AA)	R_T (\AA)
Cu-Cu	0.1043×10^6	-0.4492×10^3	-0.003 26	0.0266	2.80	7.0
Cu-Zr	0.4035×10^6	-0.1050×10^4	-0.004 70	0.0411	3.01	7.5
Zr-Zr	0.1109×10^7	-0.2230×10^4	-0.006 34	0.0592	3.16	8.0

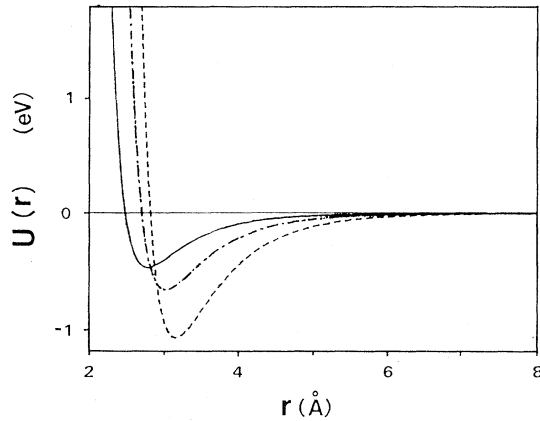


FIG. 2. Sketch of Lennard-Jones type of pair potential used in the relaxation. Solid line denotes Cu-Cu; Dashed-dotted line denotes Cu-Zr; dashed line denotes Zr-Zr.

Z_{Zr} and the short-range order parameters η_{ij} (Ref. 39) for each model, which are listed in Table II. The small values of η_{ij} indicate that there is very little chemical short-range order in these models as would be expected^{28,39} from a glass formed by an ET metal and a LT metal. We did not make any further efforts to characterize our models such as searching for the two-level tunneling centers or the estimation of their densities,³⁴ though the existence of such centers in our models cannot be ruled out. We would rather consider these models as a reasonable representation of the actual equilibrium, metastable structures of the $\text{Cu}_x\text{Zr}_{1-x}$ glasses. The atomic coordinates of the models are then used in the electronic structure calculations.

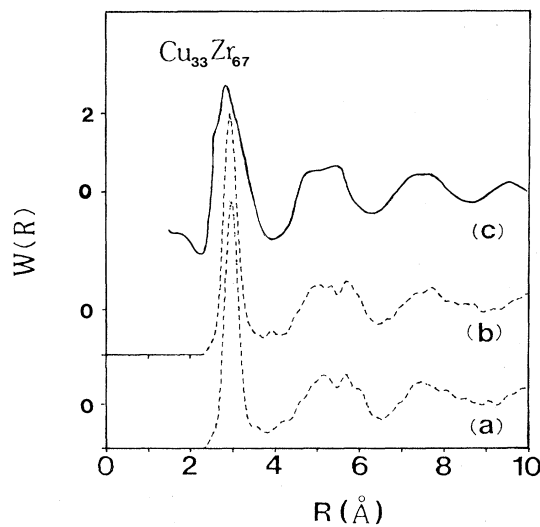


FIG. 3. Pair correlation function $W(r)$ for $\text{Cu}_{0.33}\text{Zr}_{0.67}$. (a) Relaxation by Monte Carlo method; (b) relaxation by conjugate gradient method; (c) experimental results of Ref. 27.

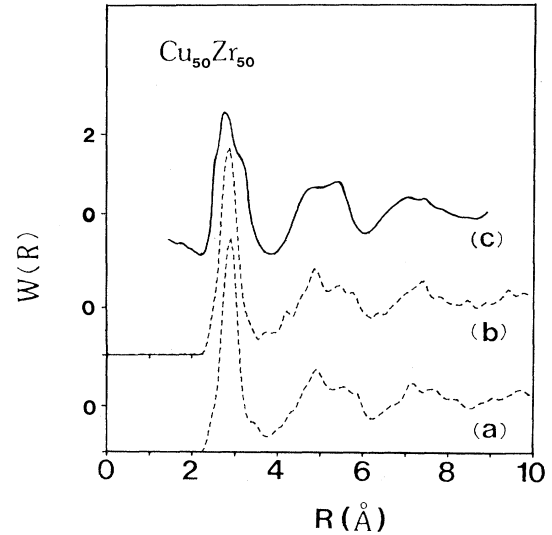


FIG. 4. Same as Fig. 3 for $\text{Cu}_{0.5}\text{Zr}_{0.5}$.

II. METHOD OF ELECTRONIC STRUCTURE CALCULATION

The first-principles OLCAO method²⁶ has been very successful in the calculation of electronic structures of disordered materials such as amorphous semiconductors,⁴⁰ insulating glasses,⁴¹ and crystals with very complex structures.⁴² We briefly outline the method in this section with special comments deemed appropriate for the metallic glass system. We start with the construction of the total charge density of the system $\rho(\vec{r})$ by superposition of atomic charge densities from atoms whose positions are defined by the coordinates of the model. In accordance with the local-density-functional theory, the exchange-correlation part of the one-electron potential can be constructed according to

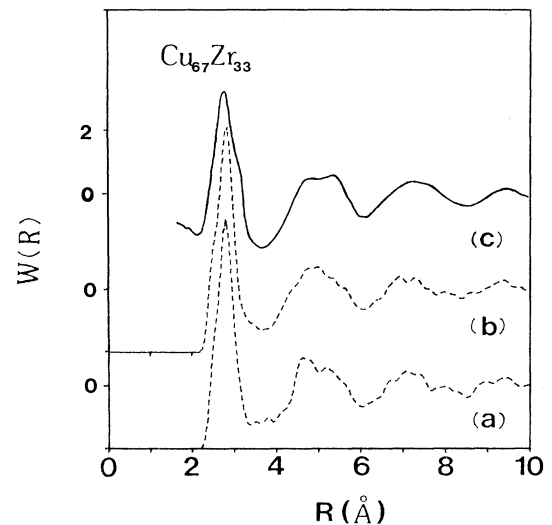


FIG. 5. Same as Fig. 3 for $\text{Cu}_{0.67}\text{Zr}_{0.33}$.

TABLE II. Some calculated characteristics of 90-atom models for $\text{Cu}_x\text{Zr}_{1-x}$. The symbols are explained in the text. Supercell lattice constant a , coordination numbers, and chemical short-range orders for $\text{Cu}_x\text{Zr}_{1-x}$ models.

x	No. of Cu atoms	No. of Zr atoms	a (Å)	Origin atom				η_{AA}	η_{BB}	η_{AB}
					Cu	Zr	Total			
0.33	30	60	12.152	Cu	3.9 ± 1.6	7.6 ± 1.4	11.6 ± 0.9	0.06	0.02	-0.03
				Zr	3.8 ± 1.6	8.6 ± 1.6	12.4 ± 0.9			
0.50	45	45	11.664	Cu	5.9 ± 2.1	5.8 ± 1.8	11.6 ± 1.0	0.05	0.04	-0.04
				Zr	5.8 ± 1.9	6.8 ± 1.6	12.6 ± 1.0			
0.67	60	30	11.294	Cu	8.1 ± 1.7	4.2 ± 1.2	12.3 ± 1.0	0.03	0.06	-0.05
				Zr	8.5 ± 2.0	5.2 ± 1.3	13.6 ± 1.2			

$$V_{\text{EC}}(\vec{r}) = -\frac{3}{2}\alpha[3\rho(\vec{r})/\pi]^{1/3}, \quad (3)$$

$$\rho(\vec{r}) = \sum_l \rho^A(\vec{r} - \vec{R}_l),$$

where α is the exchange parameter and $\rho^A(\vec{r})$ is the charge density of atom A at \vec{R}_l . For the sake of computational convenience, we decompose $V_{\text{EC}}(\vec{r})$ into localized functions $V_{\text{EC}}^A(\vec{r})$ centered at each atomic site by a numerical fitting procedure so that they add up to the $V_{\text{EC}}(\vec{r})$ given by (3). Since the Coulomb part of the potential $V_{\text{Cl}}(\vec{r})$ is a simple superposition of Coulomb potentials of each atom:

$$V_{\text{Cl}}(\vec{r}) = \sum_l V_{\text{Cl}}^A(\vec{r} - \vec{R}_l), \quad (4)$$

$$V_{\text{Cl}}^A = -\frac{Z_A}{r} + \int \frac{\rho^A(\vec{r}')}{|\vec{r} - \vec{r}'|} d\vec{r}',$$

where Z_A is the atomic mass number of atom A , the total one-electron potential $V(\vec{r})$ can be written as a superposition of atomiclike potentials $V^A(\vec{r})$ centered at each site:

$$V(\vec{r}) = V_{\text{Cl}}(\vec{r}) + V_{\text{EC}}(\vec{r}) = \sum_l V^A(\vec{r} - \vec{R}_l), \quad (5)$$

where

$$V^A(\vec{r}) = V_{\text{Cl}}^A(\vec{r}) + V_{\text{EC}}^A(\vec{r}). \quad (6)$$

The effective atomiclike potential $V^A(\vec{r})$ differs from the true atomic potential only in the valence region due to the presence of other atoms in the solid. The potential constructed above is generally called the "overlap of atomic charge density" (OAC) model. The OAC model has been shown⁴³ to give better results than does the simpler "overlap of atomic potential" (OAP) model. In an amorphous solid, $V^A(\vec{r})$ differs slightly from site to site because of the different local environments. For practical reasons, we averaged $V^A(\vec{r})$ over different sites of the same type of atom; thus $V^A(\vec{r})$ depends only on the atomic species and the compositional parameter x . $V^A(\vec{r})$ is numerically fitted to a functional form consisting of a sum of Gaussians,²⁶ in order to facilitate the later evaluation of multicenter integrals occurring in the Hamiltonian matrix elements. Next, we use the method of contraction to obtain a set of atomiclike orbitals $\mu_i(\vec{r})$ which are the linear combination of Gaussian type orbitals (GTO), i.e.,

$e^{-\alpha_i r^2}$ for s -type orbitals, $x e^{-\alpha_i r^2}$ for p_x orbitals, $x y e^{-\alpha_i r^2}$ for d_{xy} orbitals, etc. We first choose a convenient set of 13 Gaussian exponentials $\{\alpha_i\}$ ranging from $\alpha_1 = 0.15$ to $\alpha_{13} = 250000$, and use this set of single Gaussians as basis functions in solving the Schrödinger equation with potential $V^A(\vec{r})$. The resulting eigenvalues can be easily identified as atomiclike states^{15,25} of the atom A and the corresponding normalized eigenvector coefficients will be the coefficients of different GTO in forming $\mu_i(\vec{r})$. These contracted atomiclike orbitals are qualitatively similar to the free-atom orbitals, but are generally shorter ranged and include, to some degree, the distortion caused by other atoms in the solid. We use the same set $\{\alpha_i\}$ for contraction with Cu and Zr atoms, as well as for states of different angular momenta. This is a very important feature in our method because it greatly reduces the number of integrals which must be calculated and makes a seemingly impossible first-principles calculation for an amorphous solid manageable. A Bloch sum may be constructed from $\mu_i(\vec{r})$:

$$b_{i\alpha}(\vec{k}, \vec{r}) = \sum_{\nu} e^{i\vec{k} \cdot \vec{R}_{\nu}} \mu_i(\vec{r} - \vec{R}_{\nu} - \vec{\rho}_{\alpha}), \quad (7)$$

where \vec{R}_{ν} is the supercell lattice and $\vec{\rho}_{\alpha}$ is the position of the α th atom in the ν th cell. For a sufficiently large cell, such as those considered here, the Brillouin zone (BZ) is very small and only the case $\vec{k} = 0$ need to be considered. Effectively, our calculation is \vec{k} independent, as it should be for an amorphous solid where \vec{k} is no longer a good quantum number. With the use of a minimal basis set, the index i covers the core orbitals and the occupied valence orbitals of each atom. Since the core states are not of our prime interest, we wish to eliminate the core states from the calculation without the risk of losing any accuracy in energy eigenvalues. This is accomplished by orthogonalizing $b_{i\alpha}(\vec{k}, \vec{r})$ to all the core Bloch sums of all the other atoms.²⁶ We now use $b'_{i\alpha}(\vec{k}, \vec{r})$ to denote an orthogonalized Bloch sum in which i covers only the occupied valence orbitals. These are $4s$, $4p_x$, $4p_y$, $4p_z$, $3d_{xy}$, $3d_{yz}$, $3d_{zx}$, $3d_{x^2-y^2}$, and $3d_{3z^2-x^2}$ for Cu atoms and $5s$, $5p_x$, $5p_y$, $5p_z$, $4d_{xy}$, $4d_{yz}$, $4d_{zx}$, $4d_{x^2-y^2}$, and $4d_{3z^2-x^2}$ for Zr atoms. The electron states are obtained by solving the 810×810 secular equation:

$$|H'_{i\alpha, j\beta}(\vec{k}) - S'_{i\alpha, j\beta}(\vec{k})E(\vec{k})| = 0 \quad (8)$$

at $\vec{k}=0$. Here, $H'_{i\alpha,j\beta}$ and $S'_{i\alpha,j\beta}$ are the Hamiltonian and overlap matrix elements in the orthogonalized space, respectively:

$$S'_{i\alpha,j\beta} = \langle b'_{i\alpha}(\vec{k}) | b'_{j\beta}(\vec{k}) \rangle, \quad (9)$$

$$H'_{i\alpha,j\beta} = \langle b'_{i\alpha}(\vec{k}) | [-\nabla^2 + V(\vec{r})] | b'_{j\beta}(\vec{k}) \rangle. \quad (10)$$

We let $\psi_n(\vec{r})$ be a normalized electron wave function obtained from the solution of (8). We can divide this one electron among different orbitals of different atoms by using Mulliken's population-analysis scheme:⁴⁴

$$1 = \int |\psi_m(\vec{r})|^2 d\vec{r} = \sum_{\alpha,i} \rho_{i,\alpha}^m, \quad (11)$$

where

$$\rho_{i,\alpha}^m = \sum_{j,\beta} C_{i,\alpha}^{m*} C_{j,\beta}^m S'_{i\alpha,j\beta} \quad (12)$$

and $C_{i,\alpha}$ is the eigenvector coefficient of the state m . The fractional charge $\rho_{i,\alpha}^m$ can be used to define the LI for the state m according to

$$L_m = \sum_{\alpha,i} (\rho_{i,\alpha}^m)^2. \quad (13)$$

L_m is a measure of the spread of the charge for the state m among the different atomic sites α and orbitals i . For an extended state, L_m is close to $1/N$ where N is the dimension of the matrix equation (8). The $\rho_{i,\alpha}^m$ can also be used to partition the DOS curves into partial components that correspond to different atoms and different orbitals of each atom. The partial DOS (PDOS) and LI are essential in discussing the nature of the electron states in metallic glasses. $\rho_{i,\alpha}^m$ can also be used to define an approximate effective charge, Q_α^* , assigned to each atom according to

$$Q_\alpha^* = \sum_{\substack{m,i \\ \text{occup}}} \rho_{i,\alpha}^m. \quad (14)$$

IV. RESULTS

The electronic structures of $\text{Cu}_x\text{Zr}_{1-x}$ are calculated for three values of x , namely $x=0.33$, 0.50 , and 0.67 , using the 90-atom models discussed in Sec. II. The exchange parameters are chosen to be 0.81 for Cu and 0.78 for Zr, because the use of these values for the exchange potential and the use of the same minimal basis set yield very satisfactory band structures of elemental Cu and Zr. In Fig. 6 we display the band structure and DOS of the fcc Cu from such a calculation. These results are comparable to some of the best existing self-consistent calculations.⁴⁵ It is gratifying that a simple nonself-consistent OLCAO calculation involving diagonalization of only 9×9 matrix equations can give rise to a band structure of high quality. By a judicious choice of exchange parameters for both Cu and Zr, we have, to a certain extent, partially taken into account the effects of self-consistency of potential in our calculation.

The DOS and PDOS calculated for the three values of x are shown in Figs. 7–9, respectively. These curves are in good agreement with the experimental x-ray photoemission spectroscopy (XPS) curves with comparable

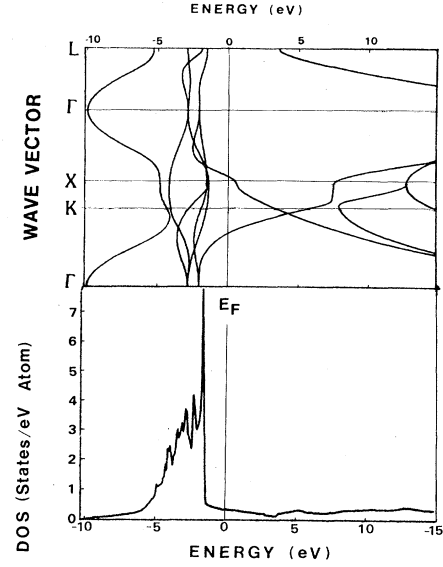


FIG. 6. Band structure and DOS of fcc Cu calculated by OLCAO method using an effective OAC atomiclike potential V_{Cu} and a minimal basis.

values of x ,²³ although the calculated peak positions E_p appear to be about 0.4–0.5 eV too low. From the PDOS curves, it is clear that the minimum in the DOS curve is formed by the crossing over of the Cu 3d and Zr 4d bands. The location of this minimum E_{min} shifts to higher binding energy as x is increased in agreement with experimental observation.^{23,46} However, the experimental XPS curves show a stronger concentration dependence of E_p and E_{min} than does the present calculation. There is

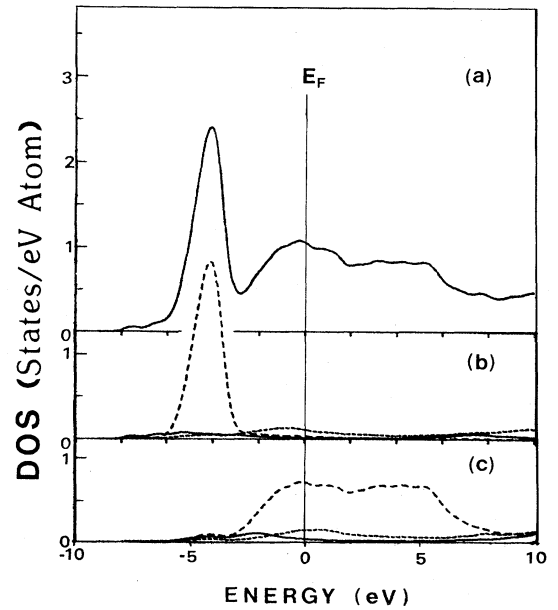
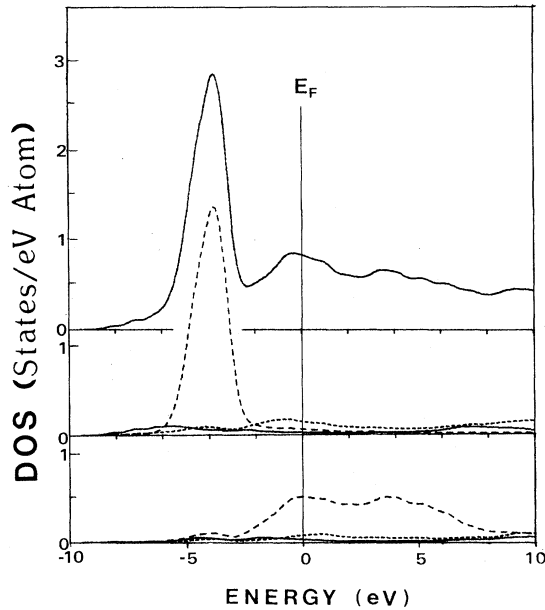


FIG. 7. Calculated DOS for $\text{Cu}_{0.33}\text{Zr}_{0.67}$. (a) Total DOS. (b) PDOS of Cu: Solid line denotes Cu 4s; dashed line denotes Cu 3d; dotted line denotes Cu 4p. (c) PDOS of Zr: Solid line denotes Zr 5s; dashed line denotes Zr 4d; dotted line denotes Zr 5p.

FIG. 8. Same as Fig. 7 for $\text{Cu}_{0.5}\text{Zr}_{0.5}$.

no evidence of the spurious substructures in the DOS curves which appear in other theoretical calculations.^{8,10,12} To meet a more stringent test on the accuracy of our calculation, we computed the DOS at E_f , $N(E_f)$ for the three compositional values of x and these are listed in Table III together with other important quantities calculated. These values of $N(E_f)$ are also decomposed into different atomic and orbital components. In Fig. 10 we plot the calculated $N(E_f)$ of $\text{Cu}_x\text{Zr}_{1-x}$ as a function of x together with several experimentally determined values.^{14,15,17,22} These are the bare DOS's at E_f obtained from the low-temperature specific heat and superconducting temperature data, converted by using McMillan's formula.⁴⁷ It is clear that the calculated values of $N(E_f)$ are

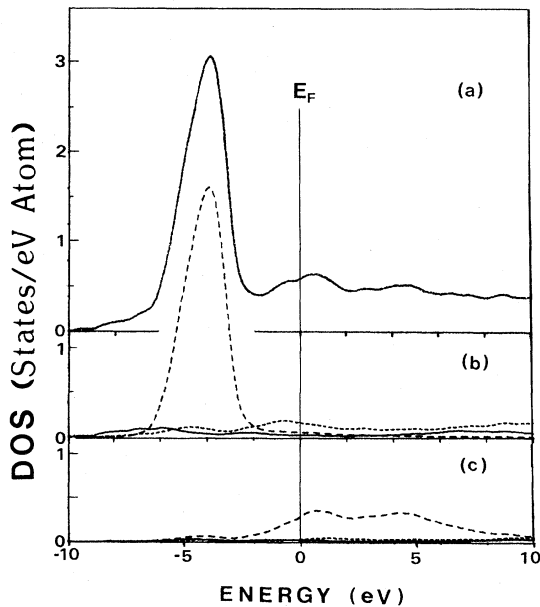
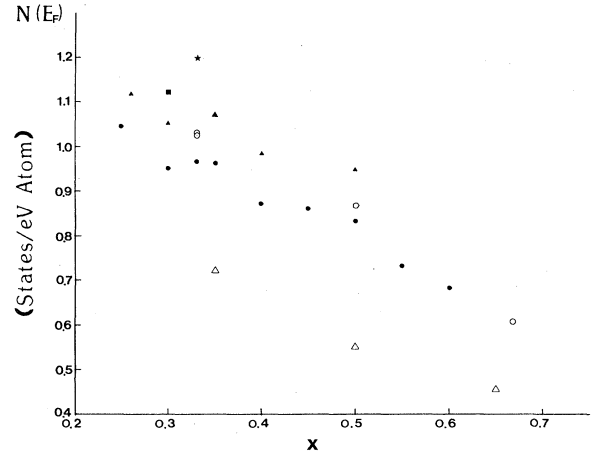
FIG. 9. Same as Fig. 7 for $\text{Cu}_{0.67}\text{Zr}_{0.33}$.

FIG. 10. Plot of $N(E_f)$ as a function of x . Experimental data: ● denotes Ref. 14; △ denotes Ref. 17; ■ denotes Ref. 15; * denotes Ref. 22. Theoretical calculation: ○ denotes present work; △ denotes Ref. 10.

in excellent agreement with experiments. On the other hand, recent calculations by Fujiwara¹⁰ gave $N(E_f)$ values about 35% too low. From the values listed in Table III, we observe that at low x , $N(E_f)$ is dominated by Zr 4d states but with a non-negligible contribution of about 13% from Cu states as well. At a higher Cu content ($x=0.67$), $N(E_f)$ is about 43% for Cu states. Both Cu 4s, Cu 4p and Zr 5s, Zr 5p make small but non-negligible contributions to $N(E_f)$. The ratios of Zr 4d states to Zr 5s and Zr 5p states are consistent with relative magnitudes obtained from susceptibility measurements.¹⁸ The

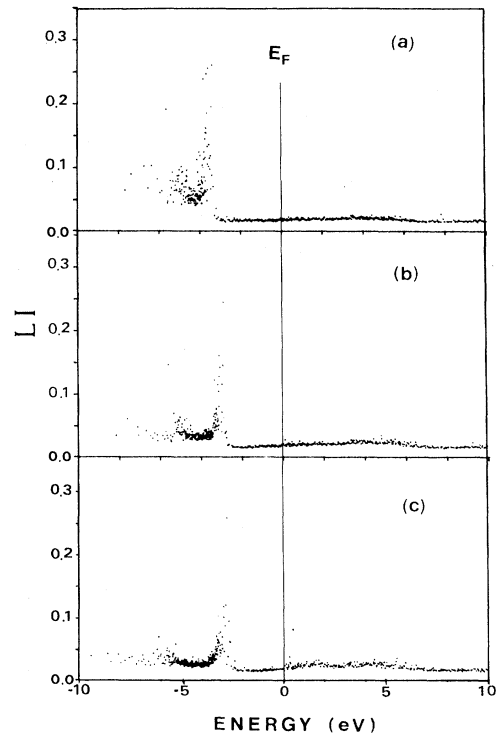


FIG. 11. Calculated LI of $\text{Cu}_x\text{Zr}_{1-x}$ glasses: (a) $x=0.33$, (b) $x=0.50$, and (c) $x=0.67$.

TABLE III. Some calculated electronic properties of $\text{Cu}_x\text{Zr}_{1-x}$. The symbols are explained in the text.

x	E_p (eV)	E_{\min} (eV)	Effective charge (electrons)		Charge transfer per atom (electrons)		$N(E_F)$ (states/eV atom)						
			Q_{Cu}^*	Q_{Zr}^*	$\Delta Q^*/\text{Cu}$	$\Delta Q^*/\text{Zr}$	Cu 4s	Cu 4p	Cu 3d	Zr 5s	Zr 5p	Zr 4d	Total
0.33	-4.12	-2.81	11.98	3.51	0.98	-0.49	0.014	0.101	0.026	0.031	0.156	0.713	1.04
0.50	-3.81	-2.40	11.83	3.17	0.83	-0.83	0.012	0.114	0.050	0.028	0.078	0.577	0.86
0.67	-4.10	-1.80	11.79	2.42	0.79	-1.58	0.019	0.181	0.060	0.028	0.029	0.289	0.61

average effective charges Q_{Cu}^* and Q_{Zr}^* are also listed in Table III. There is a considerable amount of charge transfer from the Zr atoms to Cu atoms. For $x=0.5$, an average of 0.83 electrons are transferred from a Zr atom to a Cu atom. Because the effective charges are calculated according to a Mulliken's scheme⁴⁴ which is of limited validity in metallic systems, and because the present calculation is not fully self-consistent, the amount of charge transfer quoted above should be viewed with caution.

To ascertain the nature of electron states in $\text{Cu}_x\text{Zr}_{1-x}$, we calculated the LI of each state according to (13). These are plotted in Fig. 11. The following observations can be made. (1) For low Cu content, all Cu states are localized. When the Cu content is increased, only the states near the Cu 3d band edges are localized. (2) The Zr states are generally delocalized, although there is a tendency to increase the LI when the Zr content becomes small. The relative differences in LI between Cu and Zr states can be attributed to the much wider Zr 4d band (10–15 eV) as compared to the Cu 3d band (3–4 eV). (3) The states at E_f are not localized. However, as the Zr concentration is decreased, the Fermi level moves closer to the edge of the Zr 4d band, and the states at the vicinity of E_f start to show some signs of increased localization. This fact is exemplified in Fig. 12 in which we plot the LI for states

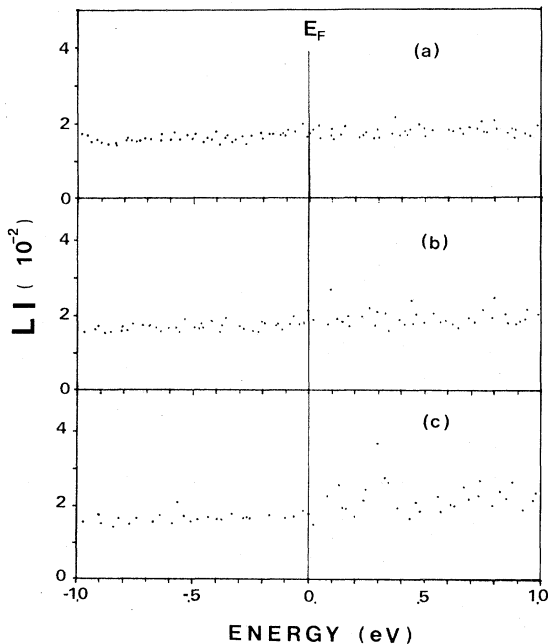


FIG. 12. Same as Fig. 11, but only for states 1 eV above and below E_f .

within 1 eV above and below E_f in an enlarged scale. In comparison with highly localized Cu states, these states near E_f can still be judged to be relatively delocalized. From these results, it is fair to conclude that it is very unlikely to have states at E_f highly localized for any other values of x in the $\text{Cu}_x\text{Zr}_{1-x}$ series.

V. DISCUSSION

We have calculated the electronic structures of $\text{Cu}_x\text{Zr}_{1-x}$ glasses using a first-principles method. Our results provide three levels of information about the electron states in metallic glasses, namely (1) the DOS, (2) the quantitative value of the DOS at E_f , and (3) the nature of electron localization in such a glass. The overall agreement with experimental measurements is very good. Two questions that have been constantly raised with regard to such theoretical calculation are the following: (1) Is the calculation based on a single-structure model for each x representative of the actual electronic structure of the glass? (2) Is the cubic cell consisting of 90 atoms sufficiently large to represent an amorphous solid? To address the first question, we made an additional calculation on $\text{Cu}_{0.33}\text{Zr}_{0.67}$ based on another structural model independently constructed. The PCF calculated from these two models are almost the same. The DOS curves calculated using these two different models of same x are compared in Fig. 13(a). There is hardly any difference in the two curves, indicating that the results from a single-model calculation are indeed quite representative. To answer the second question, we note that if the cell is sufficiently large, the corresponding BZ will be sufficiently small and the DOS based on the eigenvalues obtained by diagonalization of matrix equation (8) at the center of the BZ and at the corner of the BZ should be the same. Figure 13(b) shows the DOS of $\text{Cu}_{0.33}\text{Zr}_{0.67}$ obtained at $\vec{k}=(0,0,0)$ and $\vec{k}=(2\pi/a)(1,1,1)$, respectively. The spectra from these two calculations are almost indistinguishable, especially for states below E_f . We thus conclude that, as far as electronic DOS is concerned, a 90-atoms model is sufficiently large for a system such as $\text{Cu}_x\text{Zr}_{1-x}$.

There are several aspects of our calculation which differ from other theoretical approaches. First, by using a periodic model of definite size, the density of the model is always correct, in contrast to cluster type of models^{6,8,10,34} in which the density may not agree with the experimentally measured value. Second, because the actual atomic position of each atom enters into the calculation rather than just partial structure factors, the disorder in the metallic glass system is treated at a microscopic level. Third, due to the first-principles nature of the calculation, the effect of potential fluctuation and the short-range order of each

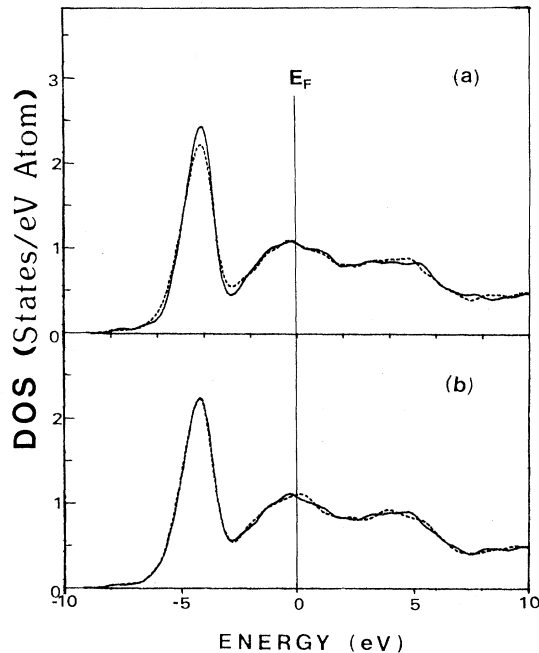


FIG. 13. (a) Total calculated DOS for $\text{Cu}_{0.33}\text{Zr}_{0.67}$ using two independent structural models. (b) Total calculated DOS for $\text{Cu}_{0.33}\text{Zr}_{0.67}$ obtained from $\vec{k}=(0,0,0)$ and $\vec{k}=(2\pi/a)(1,1,1)$, where a is the supercell lattice constant.

individual atom are fully taken into account. This, in conjunction with the use of large unit cell, enables us to quantitatively analyze each state in terms of its LI. Fourth, there is no assumption in our theory which makes it applicable only to weak scattering cases; the method is completely general with regard to different types of glassy systems, and there are no intrinsic limitations on the number of atomic components that may be present. Last, full self-consistent-field calculation may be desirable, but in practice because of the large number of atoms involved, it is not economically feasible to perform them. It is much more efficient to construct $V^A(\vec{r})$ carefully to yield good band structures of the elemental crystals before they are used in the metallic glass calculations.

The present calculation offers no detailed information about the transport properties in $\text{Cu}_x\text{Zr}_{1-x}$ glasses other than those inferred from the nature of the electron localization at the Fermi surface. If localization is going to weaken superconductivity in $\text{Cu}_x\text{Zr}_{1-x}$, a decrease in T_c as x is increased may be due to two factors: (1) the de-

crease of $N(E_f)$ and (2) the slight increase of the LI for states near E_f . With regard to the stability of glass formation, we may conjecture that the wide compositional range x for glasses formed by an ET metal and LT metal may be associated with the delocalization of electron states in the vicinity of E_f in such glasses. Nagel and Tauc,⁴⁸ based on a nearly-free-electron model, had argued that the stability of a metallic glass should be linked to the location of E_f at a local minimum in the DOS curves. Such is not the case for $\text{Cu}_x\text{Zr}_{1-x}$, since from Figs. 7–9, E_f is located near a broad maximum in DOS for all x . The results of our localization calculation are certainly in agreement with the analytic theory of disordered systems based on model Hamiltonians.⁴⁹ General theories addressing the electron localization in metallic glasses have appeared recently.^{50,51} Girvin and Jonson⁵⁰ argued that coupling of phonon and localized electrons may actually increase the electron mobility, and such a mechanism could be the source of Mooij correlation⁵² between the resistivity and its temperature coefficient. Because of the complicated interplay of many competing factors such as the strength of scattering, the bandwidth of each orbital component of each atom, and the amount of charge transfer that may be involved in an amorphous environment, it is difficult to predict the nature of electron localization at a Fermi level for any particular system without making detailed calculations such as those demonstrated in this paper. It therefore becomes necessary to make detailed calculations on various metallic glass systems and to correlate the results with a variety of experimental observations. Such information will certainly aid the development of a consistent theory for the electronic processes in metallic glasses. Since explicit wave functions are obtained in our calculation, it may be possible to study the conductivity of metallic glasses along the line of the Kubo-Greenwood formula⁵³ or its modified simpler forms⁵⁴ without resorting to Ziman's theory, which appears to be the only presently available theory for theoretical interpretation of many transport data on metallic glasses.

ACKNOWLEDGMENTS

The work at University of Missouri–Kansas City (UMKC) is supported by the UMKC Research Council, the Weldon Spring Endowment Fund, and in part by U. S. Department of Energy Contract No. DE-AC020-79ER10462.

¹See, for example, *Glassy Metals I* edited by H.-J. Güntherodt and H. Beck (Springer, New York, 1981).

²S. R. Nagel, *Adv. Chem. Phys.* **51**, 227 (1982); U. Mizutani, *Prog. Mater. Sci.* (to be published).

³M. Ziman, *Philos. Mag.* **6**, 1031 (1961).

⁴T. E. Faber and J. M. Ziman, *Philos. Mag.* **11**, 153 (1965).

⁵P. J. Cote and L. V. Meisel, *Phys. Rev. Lett.* **39**, 102 (1977); L. V. Meisel and P. J. Cote, *Phys. Rev. B.* **16**, 2978 (1977).

⁶B. Delley, D. Ellis, and A. J. Freeman, *J. Phys. (Paris) Colloq.* **41**, C8-437 (1980).

⁷J. Kübler, K. H. Bennemann, R. Lapka, F. Rösel, P. Olehafen, and H.-J. Güntherodt, *Phys. Rev. B* **23**, 5176 (1981); V. L. Moruzzi, P. Oelhafen, A. R. Williams, R. Lapka, H.-J. Güntherodt, and J. Kübler, *ibid.* **27**, 2049 (1983).

⁸R. H. Fairlie, W. M. Temmeman, and B. L. Gyorffy, *J. Phys. F* **12**, 1641 (1982).

⁹R. P. Messmer, *Phys. Rev. B* **23**, 1616 (1981).

¹⁰T. Fujiwara, *J. Phys. F* **12**, L251 (1982); **12**, 661 (1982).

¹¹P. Nicholson, L. Huisman, L. Schwartz, A. Bansil, and R. Prasad, *Solid State Commun.* **46**, 891 (1983).

- ¹²S. Frota-Pessôa, Phys. Rev. B **28**, 3753 (1983).
- ¹³R. W. Cochrane, J. Destry, and M. Trudeau, Phys. Rev. B **27**, 5955 (1983).
- ¹⁴Z. Altounian and J. O. Strom-Olsen, Phys. Rev. B **27**, 4149 (1983).
- ¹⁵M. Tenhover and W. L. Johnson, Phys. Rev. B **27**, 1610 (1983).
- ¹⁶L. E. McNeil and D. Lazarus, Phys. Rev. B **27**, 6007 (1983).
- ¹⁷K. Samwer and H. v. Löhneysen, Phys. Rev. B **26**, 107 (1982).
- ¹⁸H. J. Eifert, B. Elschner, and K. H. J. Buschow, Phys. Rev. B **25**, 7441 (1982).
- ¹⁹D. Greig and M. A. Howsen, Solid State Commun. **42**, 729 (1982).
- ²⁰G. Fritsch, J. Willer, A. Wildermuth, and E. Lüscher, J. Phys. F **12**, 2965 (1982); J. Willer, G. Fritsch, and E. Lüscher, J. Non-Cryst. Solids **46**, 321 (1981).
- ²¹P. Esquinazi, M. E. de la Cruz, A. Ridner, and F. de la Cruz, Solid State Commun. **44**, 941 (1982); J. Guimpel and F. de la Cruz, *ibid.* **44**, 1045 (1982).
- ²²P. Garoche and J. J. Veysie, J. Phys. (Paris) Lett. **42**, L365 (1981); P. Garoche, Y. Calva, W. Cheng, and T. T. Veysie (unpublished).
- ²³P. Oelhafen, E. Hauser, H.-J. Güntherodt, and K. H. Bennemann, Phys. Rev. Lett. **43**, 1134 (1979); P. Oelhafen, E. Hauser, and H.-J. Güntherodt, Solid State Commun. **35**, 765 (1980).
- ²⁴A. Amamon and G. Krill, Solid State Commun. **28**, 957 (1978).
- ²⁵F. R. Sofran, G. R. Gruzalski, J. W. Weymouth, D. J. Sellmyer, and B. C. Giessen, Phys. Rev. B **14**, 2160 (1976).
- ²⁶W. Y. Ching and C. C. Lin, Phys. Rev. B **12**, 5536 (1975); **16**, 2989 (1977).
- ²⁷S. S. Jaswal, W. Y. Ching, D. J. Sellmyer, and P. Edwardson, Solid State Commun. **42**, 247 (1982); S. S. Jaswal and W. Y. Ching, Phys. Rev. B **26**, 1064 (1982).
- ²⁸H. S. Chen and Y. Waseda, Phys. Status Solidi A **51**, 593 (1979).
- ²⁹T. Kudo, T. Mizoguchi, N. Watanabe, N. Niimura, M. Misawa, and K. Suzuki, J. Phys. Soc. Jpn. **45**, 1773 (1978).
- ³⁰L. A. Davis, Y. T. Yeow, and P. M. Anderson, J. Appl. Phys. **53**, 4834 (1982).
- ³¹Z. Altounian, Tu Guo-hua, and J. O. Strom-Olsen, J. Appl. Phys. **53**, 4755 (1982).
- ³²D. S. Boudreaux and J. M. Gregor, J. Appl. Phys. **48**, 5057 (1977).
- ³³S. Kobayashi, K. Maeda, and S. Takeuchi, J. Phys. Soc. Jpn. **48**, 1147 (1980).
- ³⁴R. Harris and L. J. Lewis, Phys. Rev. B **25**, 4997 (1982).
- ³⁵R. Fletcher and M. J. D. Powell, Comput. J. **6**, 163 (1963).
- ³⁶N. Metropolis, A. W. Rosenbluth, M. N. Rosenbluth, A. H. Teller, and E. Teller, J. Chem. Phys. **21**, 1087 (1953).
- ³⁷T. Fujiwara, H. S. Chen, and Y. Waseda, J. Phys. F **13**, 97 (1983).
- ³⁸J. Hafner, Phys. Rev. B **27**, 678 (1983).
- ³⁹G. S. Gargill III and F. Spaepen, J. Non-Cryst. Solids **43**, 91 (1981).
- ⁴⁰W. Y. Ching and C. C. Lin, Phys. Rev. B **12**, 5536 (1975); **16**, 2989 (1977).
- ⁴¹S. Y. Ren and W. Y. Ching, Phys. Rev. B **23**, 5454 (1981); W. Y. Ching and S. Y. Ren, *ibid.* **24**, 5788 (1981); W. Y. Ching, A. D. Murray, D. J. Lam, and B. W. Veal, *ibid.* **28**, 4724 (1983).
- ⁴²W. Y. Ching, Phys. Rev. Lett. **46**, 607 (1981); Phys. Rev. B **26**, 6632 (1982).
- ⁴³W. Y. Ching, L. W. Song, and S. S. Jaswal, Bull. Am. Phys. Soc. **28**, 484 (1983); J. Non-Cryst. Solids **61-62**, 1207 (1984).
- ⁴⁴R. S. Mulliken, J. Chem. Phys. **23**, 1833 (1955).
- ⁴⁵V. L. Moruzzi, J. F. Janak, and A. R. Williams, *Calculated Electronic Properties of Metals* (Pergamon, New York, 1978).
- ⁴⁶P. Oelhafen, in *Glassy Metals II*, edited by H.-J. Güntherodt and H. Beck (Springer, New York, 1983).
- ⁴⁷W. L. McMillan, Phys. Rev. **167**, 331 (1967).
- ⁴⁸S. R. Nagel and J. Tauc, Phys. Rev. Lett. **35**, 380 (1975).
- ⁴⁹P. W. Anderson, Phys. Rev. **109**, 1492 (1958).
- ⁵⁰S. M. Girvin and M. Jonson, Phys. Rev. B **22**, 3583 (1980).
- ⁵¹Y. Imry, Phys. Rev. Lett. **44**, 469 (1980).
- ⁵²J. J. Mooij, Phys. Status Solidi A **17**, 521 (1973).
- ⁵³R. Kubo, Can. J. Phys. **34**, 1274 (1956); D. A. Greenwood, Proc. Phys. Soc. London **71**, 585 (1973).
- ⁵⁴S. Datta, Phys. Rev. Lett. **44**, 828 (1980).